JACS
JOURNAL OF THE AMERICAN CHEMICAL SOCIETY
pubs.acs.org/JACS
Article

Palladium-Catalyzed Asymmetric Hydrogenolysis of Epoxides

Xiang Li, Qianqian Shi, Qing-Xian Xie, Huan Jing, Chang-Bin Yu,* Yu Lan,* and Yong-Gui Zhou*

Cite This: J. Am. Chem. Soc. 2025, 147, 43560−43570
Read Online
ACCESS | Metrics & More | Article Recommendations | Supporting Information

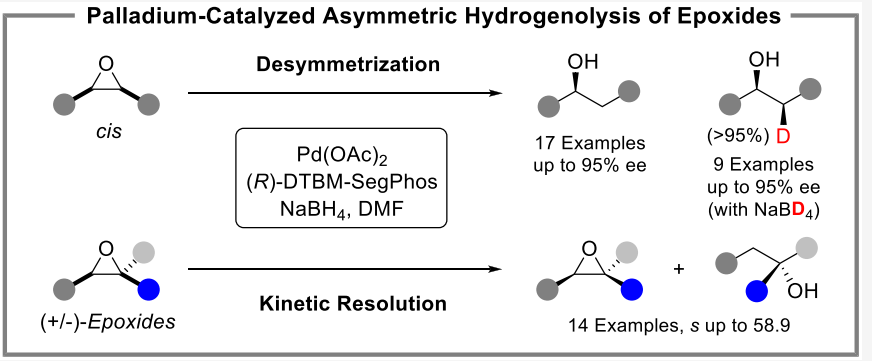

ABSTRACT: Hydrogenolysis is one of the fundamental transformations in organic synthesis. Despite numerous studies in this field over the last few decades, asymmetric C−O bond hydrogenolysis remains less explored. The enantioselective hydrogenolysis of epoxides catalyzed by transition metals can usually provide high-value-added chiral alcohols. However, β-H elimination and difficulty in stereoselective control are the main challenges. Herein, we successfully realized the palladium-catalyzed asymmetric hydrogenolysis of C(sp^3)−O bonds of epoxides by strategies including the introduction of borane reagents promoting fast hydrogen transfer from borane to the Pd(II) intermediate and bulky chiral ligands, affecting the reactivity and enantioselectivity. In addition, highly site-specific deuterated alcohols could also be synthesized with readily available sodium borodeuteride as the deuterium source. Experimental study and theoretical calculations provided deep insight into the origin of the high enantioselectivity controlled by the sterically demanding biphosphine ligand and also indicated that the hydrogenolysis undergoes a Pd(0)/Pd(II)-catalyzed process, which may shed light on a strategy for asymmetric transformation of epoxides with transition-metal complexes.

INTRODUCTION

Hydrogenolysis is one of the fundamental transformations in synthetic chemistry and is often used in the cleavage of various C-X bonds. Over the past few decades, many efficient and practical hydrogenolysis reactions have been reported by chemists.[1,2] Among them, the hydrogenolysis of C−O bonds is regarded as an attractive representative, and various types of C−O bonds have been achieved, such as ethers, alcohols, phenols, and esters.[3−5] Although there were numerous studies on nonstereoselective reactions, the application in asymmetric C−O bond hydrogenolysis remains relatively scarce. Recently, an asymmetric hydrogenolysis of C(sp^2)−O bonds was realized through desymmetrization and kinetic resolution with excellent enantioselectivities to construct axially chiral skeletons (Scheme 1a).[6] The asymmetric hydrogenolysis of C(sp^3)−O bonds was also explored. Earlier, Chan[7a] and Bakos[7b] reported that rhodium-catalyzed asymmetric hydrogenolysis of the epoxides containing activating groups (−CO_2Na), including sodium *cis*-epoxysuccinate and sodium *trans*-phenylglycidate, afforded moderate enantioselectivities and a low selectivity factor (Scheme 1b). Later, Zhang developed an elegant Pd-catalyzed hydrogenolysis kinetic resolution of α-acyloxy ketones, and high enantioselectivities were obtained with 2-aryl-substituted substrates.[8] Moreover, some formal asymmetric hydrogenolysis reactions of the C(sp^3)−O bonds were also reported.[9,10] Despite these advances, the C(sp^3)−O bond asymmetric hydrogenolysis was mainly limited in some special substrates. Therefore, the development of efficient catalytic methodologies for the asymmetric hydrogenolysis of C(sp^3)−O bonds of simple substrates is the first imperative.

Epoxides exhibit unique reactivity in ring-opening transformations and are a class of candidates with synthetic potential.[11] Asymmetric hydrogenolysis of epoxides could afford various chiral alcohols, which are useful chiral building blocks for natural products and bioactive molecules.[12] From literature reports, the C(sp^3)−O bonds in epoxides could

Received: July 25, 2025
Revised: October 31, 2025
Accepted: November 3, 2025
Published: November 11, 2025

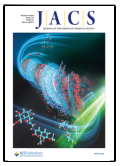

https://doi.org/10.1021/jacs.5c12776
J. Am. Chem. Soc. 2025, 147, 43560−43570

Scheme 1. Transition-Metal-Catalyzed Asymmetric Hydrogenolysis of C−O Bonds

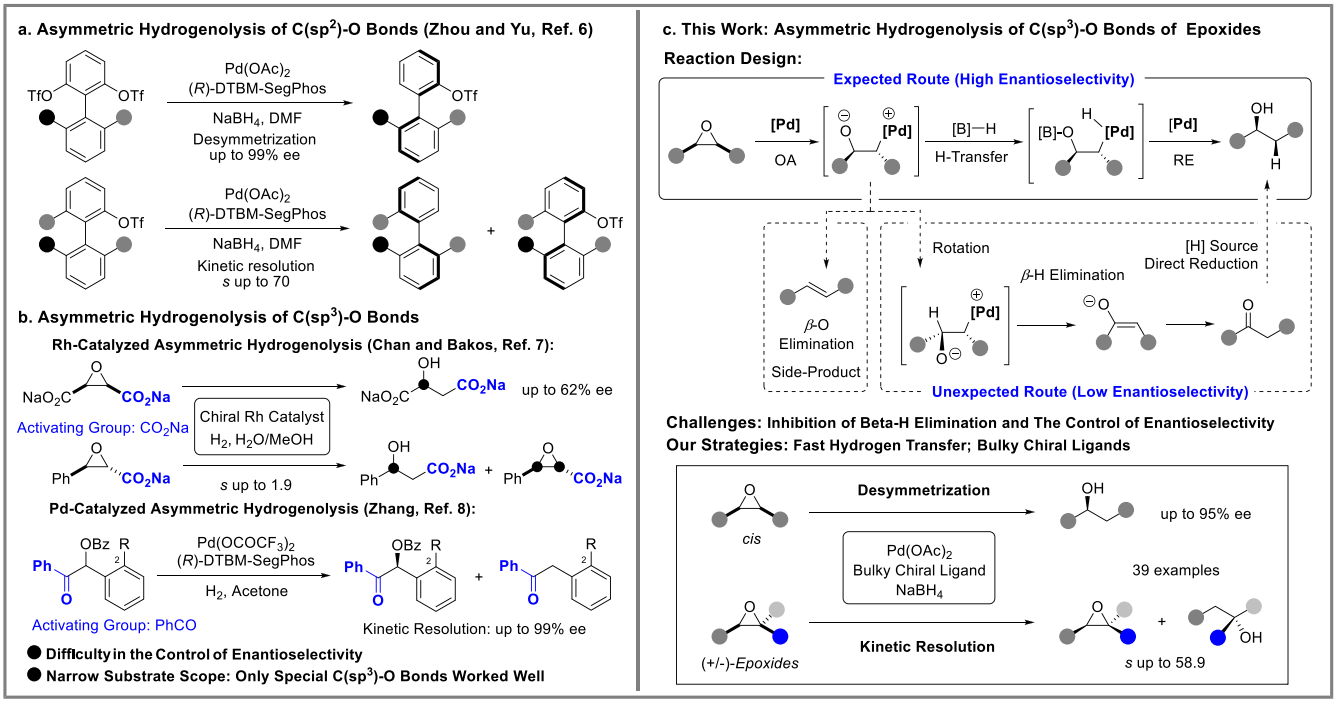

undergo oxidative addition with palladium(0) complexes to generate alkyl palladium(II) species,[13] which could be applied in asymmetric hydrogenolysis of epoxides through the capture of these alkyl palladium(II) species with the hydride reagents (Scheme 1c). However, the generated alkyl palladium(II) species easily undergo β-H elimination and are isomerized to ketones, or they may also undergo β-O elimination to olefins. The ketones could further be reduced by hydride reagents to give racemic alcohols, which is adverse for asymmetric hydrogenolysis. We speculated that (1) the fast enough hydrogen transfers from the hydride reagents, such as borane reagents with good oxyphilicity to the alkyl Pd(II) species, would suppress the unwanted β-H elimination and achieve C−O bond hydrogenolysis and (2) selecting suitable chiral ligands as the ligands can adjust the electronic and steric properties of metal centers, thus affecting the reactivity and enantioselectivity. Herein, we describe an efficient palladium-catalyzed asymmetric hydrogenolysis of simple epoxides *via* desymmetrization and kinetic resolution to construct a series of chiral alcohols and epoxides with high regioselectivities and enantioselectivities. Furthermore, the methodology can also regioselectively introduce deuterium atoms into organic molecules using commercially available sodium borodeuteride as the deuterium source. The combination of experimental and theoretical studies indicated that the asymmetric hydrogenolysis underwent a Pd(0)/Pd(II)-catalyzed process.

RESULTS AND DISCUSSION

Based on the above hypothesis, a series of condition parameters were investigated using *cis*-**1a** as the model substrate. The borane reagents were first explored. As expected, the hydrogenolysis product **2a** was successfully obtained with good yields and excellent enantioselectivities when sodium borohydride and potassium borohydride were used as hydride sources, respectively (Table 1, entries 1 and 2). Poor reactivities were observed with sodium cyanoborohydride and HBpin (entries 3 and 4). Besides, other hydride sources have also been screened. Full conversion was observed with sodium formate, giving a 25% hydrogenolysis product (**2a**) and a 75% β-H elimination product ketone (**3a**) (entry 5). Similarly, in the presence of formic acid/triethylamine or triethylsilane, trace product formation occurred, which delivered ketones (entries 6 and 7). The use of alternative solvents, including acetonitrile, toluene, and 1,4-dioxane, did not lead to any improvement in the yield or enantioselectivity (entries 8−10). The ee values decreased slightly when $Pd(acac)_2$ and $Pd(P^tBu_3)_2$ were used as palladium precursors (entries 11 and 12), and $Pd(PPh_3)_2Cl_2$ gave low activity and enantioselectivity (entry 13). Next, various axially chiral bisphosphine ligands were surveyed (entries 14−19); all delivered high activities and moderate to good ee values, except the electron-deficient chiral ligand (*S*)-DifluorPhos (**L4**), giving low activity (entry 16), which identified that ligands containing large steric hindrance and relatively rich electrons were pivotal. Considering the yield and enantioselectivity, **L1** was determined to be the optimal ligand. Lowering the temperature to 25 °C diminished the yield to 75% (entry 20). A 93% ee value was afforded when 10 mol % ligand was used, which may be ascribed to the fact that extra ligands are beneficial to stabilize the chiral palladium complexes (entries 21 and 22). The yield and enantioselectivity could also be maintained by using 1.5 equiv of sodium borohydride (entry 23). Finally, the optimal conditions were established: palladium acetate (5 mol %), (*R*)-DTBM-SegPhos (10 mol %), *N*,*N*-dimethylformamide, sodium borohydride (1.5 equiv), and 40 °C.

With the optimized conditions in hand, the exploration of the scope of this catalytic protocol was performed with *cis*-**1**, as shown in Scheme 2, where variations in substituents at the 4-position of the benzene ring were introduced and could provide hydrogenolysis products with high yields and enantioselectivities. For example, the presence of various

https://doi.org/10.1021/jacs.5c12776
J. Am. Chem. Soc. 2025, 147, 43560−43570

Table 1. Condition Optimization for Palladium-Catalyzed Asymmetric Hydrogenolysis of Epoxides

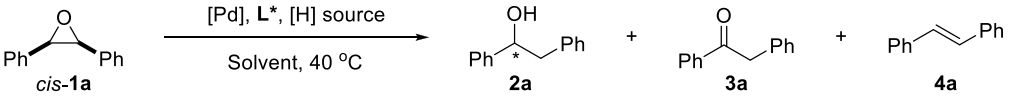

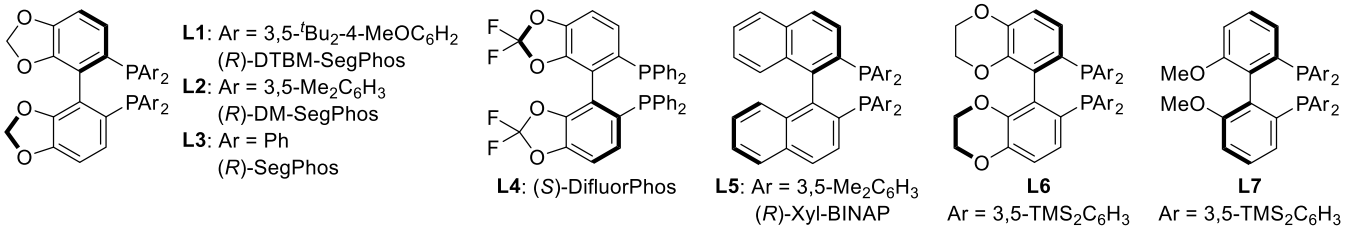

entry[a]	[H] source	solvent	[Pd]	L*	convn (%)[b]	2a yield (%)[b]	ee (%)[c]	3a yield (%)[b]	4a yield (%)[b]
1	$NaBH_4$	DMF	$Pd(OAc)_2$	L1	>95	82	91	<5	7
2	KBH_4	DMF	$Pd(OAc)_2$	L1	>95	78	92	9	6
3	$NaBH_3CN$	DMF	$Pd(OAc)_2$	L1	33	6	-	19	<5
4	HBpin	DMF	$Pd(OAc)_2$	L1	34	15	92	5	<5
5	HCO_2Na	DMF	$Pd(OAc)_2$	L1	>95	25	16	75	<5
6	HCO_2H/Et_3N	DMF	$Pd(OAc)_2$	L1	>95	5	-	95	<5
7	Et_3SiH	DMF	$Pd(OAc)_2$	L1	80	<5	-	72	<5
8	$NaBH_4$	CH_3CN	$Pd(OAc)_2$	L1	>95	78	91	<5	5
9	$NaBH_4$	toluene	$Pd(OAc)_2$	L1	>95	7	6	90	<5
10	$NaBH_4$	1,4-dioxane	$Pd(OAc)_2$	L1	95	79	18	<5	6
11	$NaBH_4$	DMF	$Pd(acac)_2$	L1	90	80	86	<5	6
12	$NaBH_4$	DMF	$Pd(P^tBu_3)_2$	L1	91	86	88	<5	<5
13	$NaBH_4$	DMF	$Pd(PPh_3)_2Cl_2$	L1	22	17	77	<5	<5
14	$NaBH_4$	DMF	$Pd(OAc)_2$	L2	>95	82	69	7	<5
15	$NaBH_4$	DMF	$Pd(OAc)_2$	L3	63	45	44	<5	<5
16	$NaBH_4$	DMF	$Pd(OAc)_2$	L4	10	<5	-	<5	<5
17	$NaBH_4$	DMF	$Pd(OAc)_2$	L5	>95	84	71	<5	<5
18	$NaBH_4$	DMF	$Pd(OAc)_2$	L6	87	76	84	<5	7
19	$NaBH_4$	DMF	$Pd(OAc)_2$	L7	94	80	83	<5	7
20[d]	$NaBH_4$	DMF	$Pd(OAc)_2$	L1	85	75	91	<5	<5
21[e]	$NaBH_4$	DMF	$Pd(OAc)_2$	L1	90	73	91	<5	7
22[f]	$NaBH_4$	DMF	$Pd(OAc)_2$	L1	>95	85	93	<5	8
23[f,g]	$NaBH_4$	DMF	$Pd(OAc)_2$	L1	>95	84	94	<5	7

[a]Reaction conditions: *cis*-**1a** (0.2 mmol), [Pd] (5.0 mol %), **L*** (7.5 mol %), [H] source (2.0 equiv), solvent (2.0 mL), 40 °C, 22 h. [b]Determined by ^1H NMR analysis using 1,3,5-trimethoxybenzene as the internal standard. [c]Determined by chiral HPLC analysis. [d]The reaction was carried out at 25 °C. [e]The amount of **L1** was 6.0 mol %. [f]The amount of **L1** was 10.0 mol %. [g]The amount of sodium borohydride was 1.5 equiv.

alkyl groups did not impact the enantioselectivity (**2b**−**2f**). Furthermore, methyloxymethyl (**2g**) was also well tolerated. Trifluoromethyl-, cyano-, and fluoro-substituted epoxides (**2h**−**2l**) worked well, and good yields and excellent enantioselectivities were obtained. An apparent steric hindrance effect was observed. The methyl group at the 2-position of the benzene ring gave low yield and enantioselectivity (**2m**), whereas high yields and enantioselectivities (**2n**, **2o**) were observed when the methyl or methoxy groups were introduced into the 3-position. The substrates with disubstituted methyl groups in the benzene ring were also investigated, both of which proceeded smoothly with good yields and excellent enantioselectivities (**2p**, **2q**). To demonstrate the utility of this methodology, the asymmetric hydrogenolysis of **1a** was carried out on a 1.0 mmol scale, smoothly providing the product (−)-**2a** with 81% yield and 93% ee. The absolute configuration of product (−)-**2a** was determined to be *S* by comparing the optical rotation value with that reported in the literature.[14]

To further demonstrate the practicality of this method, the palladium-catalyzed regioselective deuteration of epoxides *cis*-**1** was carried out with commercially available sodium borodeuteride. The results are summarized in Scheme 3. Pleasingly, the hydrogenolysis could proceed smoothly to give the deuterated alcohols with good yields and excellent enantioselectivities and diastereoselectivities, which provided a good solution to the site-specific incorporation of deuterium in organic molecules. According to the rule of the coupling constant of α-hydrogen in 1,2-diphenylpropan-1-ol, the coupling constant in *anti* is greater than that in *syn*,[15] so the absolute configuration of the deuterium-containing site of (−)-*d*-**2a** was determined as *R* by comparing the corresponding coupling constants of the α-hydrogen of the alcohol hydroxyl group in the compounds (−)-(*S*)-**2a** and (−)-*d*-**2a** (see the Supporting Information for details).

The hydrogenolysis kinetic resolution of trisubstituted epoxide (±)-**5** was further explored (Scheme 4). The reaction proceeded smoothly with (±)-**5a** under the slightly modified conditions, and the selectivity factor reached 27.8. Next, the electronic effects of R^1 were investigated. The marginal influence was observed on the *s* value with the electron-donating group or the electron-withdrawing group (**5b**, **5c**). Furthermore, the *s* value achieved 48.3 when the R^1 substituent was phenyl (±)-**5d**, and the absolute configuration of (+)-**5d** was assigned as (2*R*,3*R*) by X-ray diffraction analysis (see the

https://doi.org/10.1021/jacs.5c12776
J. Am. Chem. Soc. 2025, 147, 43560−43570

Scheme 2. Substrate Scope for the Hydrogenolysis Desymmetrization of *cis*-1

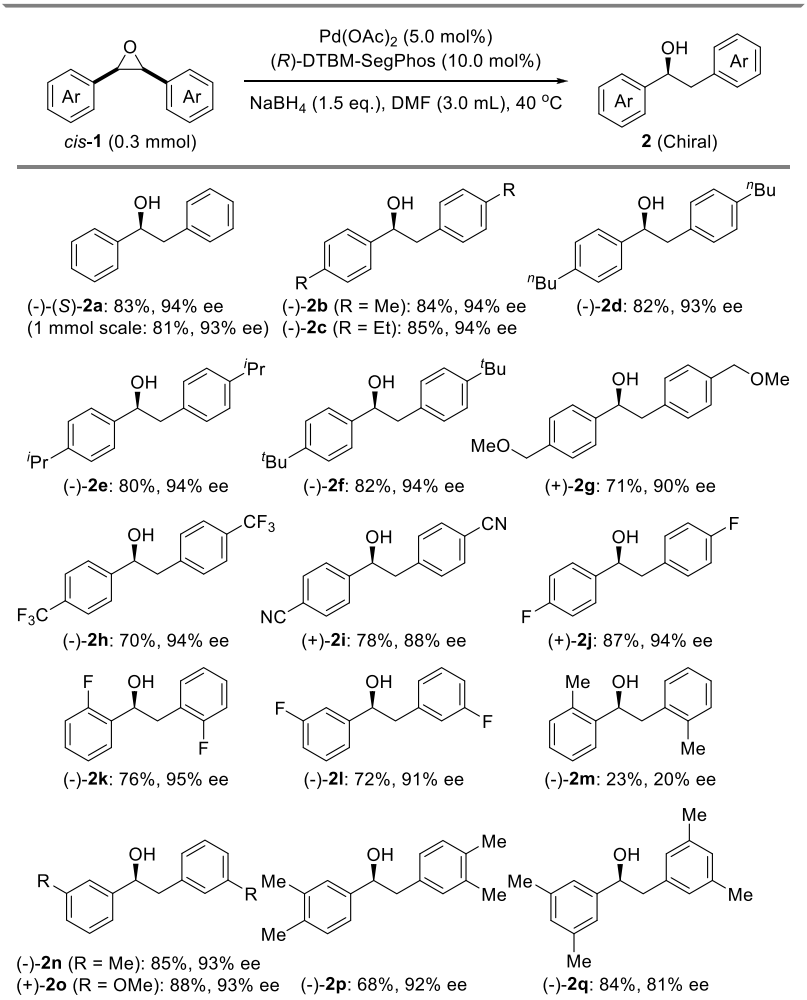

Scheme 3. Pd-Catalyzed Regioselective Deuteration

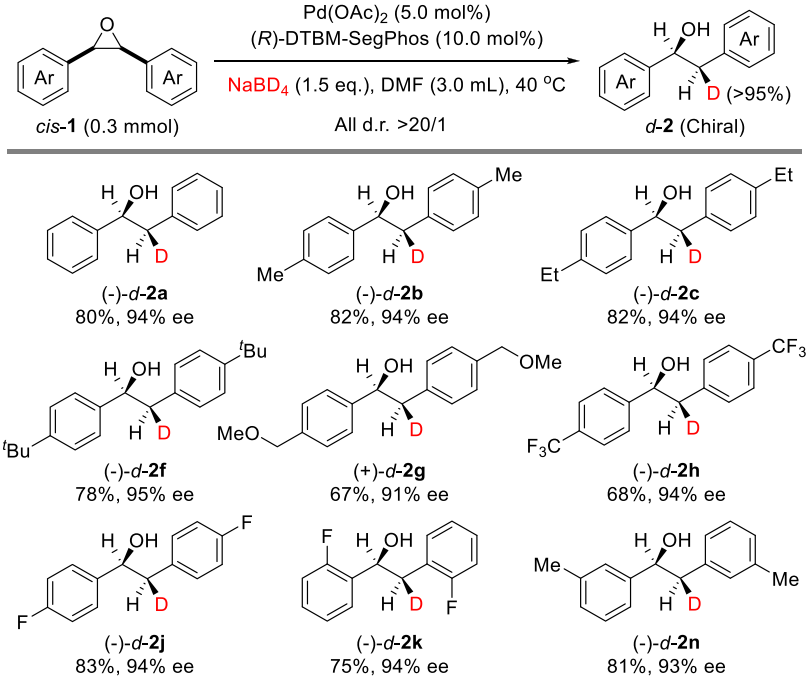

https://doi.org/10.1021/jacs.5c12776
J. Am. Chem. Soc. 2025, 147, 43560−43570

Scheme 4. Substrate Scope for the Hydrogenolysis Kinetic Resolution of (±)-5

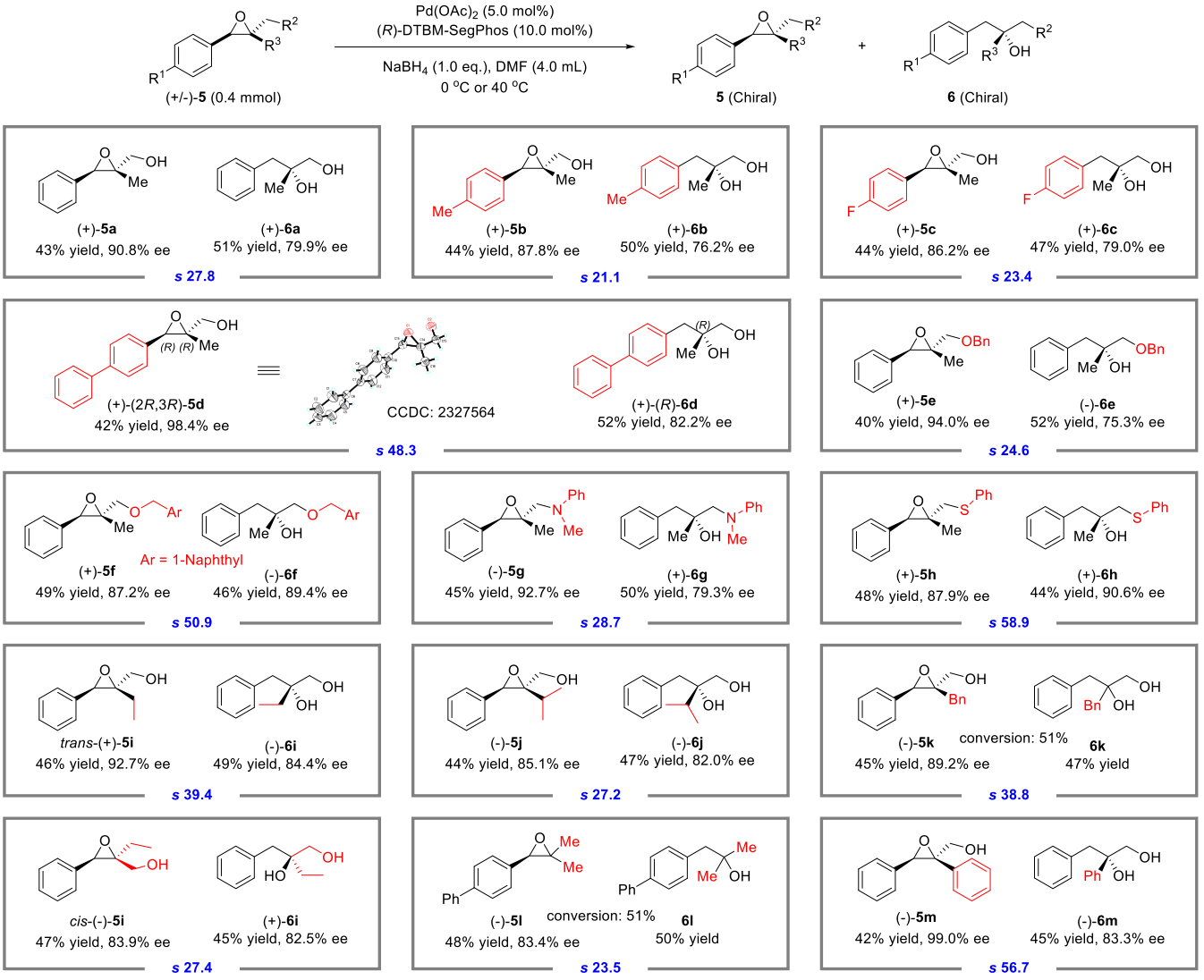

Supporting Information for details).[16] The hydroxyl-protected epoxides were also investigated, and the *s* value was up to 50.9 (**5e**, **5f**). Substrates containing nitrogen or sulfur functional groups (**5g**, **5h**) could undergo efficient hydrogenolysis and provide 28.7 and 58.9 *s* values, respectively. Various alkyl groups of R^3, such as ethyl, isopropyl, and benzyl groups, essentially did not affect the efficiency of asymmetric hydrogenolysis and gave the target products with high *s* values (**5i**−**5k**). Considering that the *s* value would be interfered by the stereoscopic configurations in the substrates, the kinetic resolution of *cis*-(±)-**5i** was also investigated. An *s* value of 27.4 was obtained, which was slightly lower than that of *trans*-(±)-**5i**. Besides, this method had good tolerance for nonfunctional simple epoxides, (±)-**5l** and 1,2-diaryl substituted (±)-**5m**, in which a single regioselective product (−)-**6m** was observed for **5m**.

Inspired by the aforementioned examples, asymmetric hydrogenolysis of other types of epoxides was explored (Scheme 5), including *trans*-2,3-diphenyloxirane, 2-butyl-3-phenyloxirane, (3-phenyl-oxiran-2-yl)methanol, and 2-phenyloxirane. Regrettably, no satisfactory results were observed; those substrates readily generated the ketone or aldehyde intermediates under the hydrogenolysis conditions, which further underwent reduction by boron reagents to afford the racemic alcohols. To explain this phenomenon, the proportion of *β*-H elimination was explored with the labeling experiments of *cis*- and *trans*-epoxide **1a** under palladium/(±)-DTBM-SegPhos/sodium borodeuteride (Scheme 5a,5b). The *β*-H elimination percentages were 3.7 and 27.2%, respectively, which indicated that *β*-H elimination of the *trans*-epoxide substrates is relatively easy, which might ascribe to the different rotation barrier; *β*-H elimination is more difficult to occur in the generated alkyl palladium(II) species from *cis*-substrates than from the *trans*-substrates. Thus, high yields and ee values could be obtained with *cis*-1,2-diaryl-substituted and trisubstituted epoxides.

Epoxides are a class of highly reactive molecules that often exhibit multiple reaction pathways.[17] In order to gain insight into the mechanism, we proposed three possible reaction processes and performed a series of verification experiments (Scheme 6). Based on the observation of the side product ketone **3a** during the condition optimization, the reaction may be a formal hydrogenolysis that *cis*-**1a** was first isomerized to the ketone **3a**, and then **3a** was directly reduced to give the product (−)-**2a**. Therefore, the ketone **3a** was employed under the standard condition, and **2a** was observed with 51% yield

https://doi.org/10.1021/jacs.5c12776
J. Am. Chem. Soc. 2025, 147, 43560−43570

Scheme 5. Other Attempts and Analyses

♥ **Unsuccessful Examples**

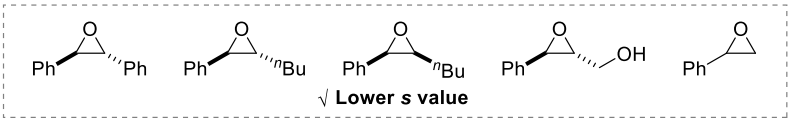

♥ **Experiments with $NaBD_4$**

(a): *cis*-**1a** → $Pd(OAc)_2$, (+/-)-DTBM-SegPhos, $NaBD_4$, DMF, 40 °C → (+/-)-*d*-**2a** + (+/-)-*d*-**2a'** + **3a** (1% yield) + **4a** (7% yield)

81% total yield, (+/-)-*d*-**2a**/(+/-)-*d*-**2a'** = 28.6/1; 3.7% *β*-H Elimination

(b): *trans*-**1a** → $Pd(OAc)_2$, (+/-)-DTBM-SegPhos, $NaBD_4$, DMF, 40 °C → (+/-)-*d*-**2a** + (+/-)-*d*-**2a'** + **3a** (8% yield)

90% total yield, (+/-)-*d*-**2a**/(+/-)-*d*-**2a'** = 3.7/1; 27.2% *β*-H Elimination

√ **Less *β*-H Elimination for *cis*-1a** √ **Reduction of Ketone 3a**

♥ ***β*-H Elimination Difference for *cis*-1a and *trans*-1a**

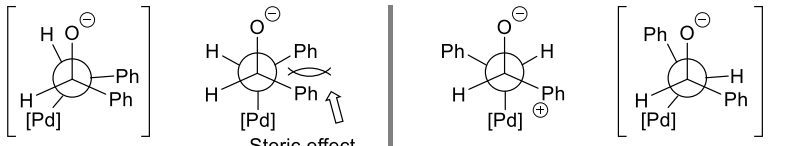

***β*-H Elimination: Hard** (from *cis*-**1a**) (from *trans*-**1a**) ***β*-H Elimination: Easy**

Scheme 6. Mechanism Study Experiments

a: **3a** → the standard conditions, 52% conversion → (-)-**2a**, 51% yield, 5% ee

b: *cis*-2,3-d_2-**1b** (94% D, 94% D) → the standard conditions, Ar = 4-MeC_6H_4 → (-)-1,2-d_2-**2b** (93% D, 94% D), 80% yield, 96% ee

c: *cis*-**1a** → $NaBH_4$, DMF, 40 °C, 22 h, 5% conversion → (+/-)-**2a**, <5%

d: *cis*-**1a** → $Pd(OAc)_2$, $NaBH_4$, DMF, 40 °C, 22 h, 13% conversion → (+/-)-**2a**, 6% yield

e: *cis*-**1a** → the standard conditions, $Pd(P^tBu_3)_2$ instead of $Pd(OAc)_2$, 83% conversion → (-)-**2a**, 78% yield, 91% ee

f: *cis*-**1a** → $Pd(P^tBu_3)_2$, $NaBH_4$, DMF, 40 °C, 22 h, 43% conversion → (+/-)-**2a** 22% yield, **3a** 6% yield, **4a** 9% yield

https://doi.org/10.1021/jacs.5c12776
J. Am. Chem. Soc. 2025, 147, 43560−43570

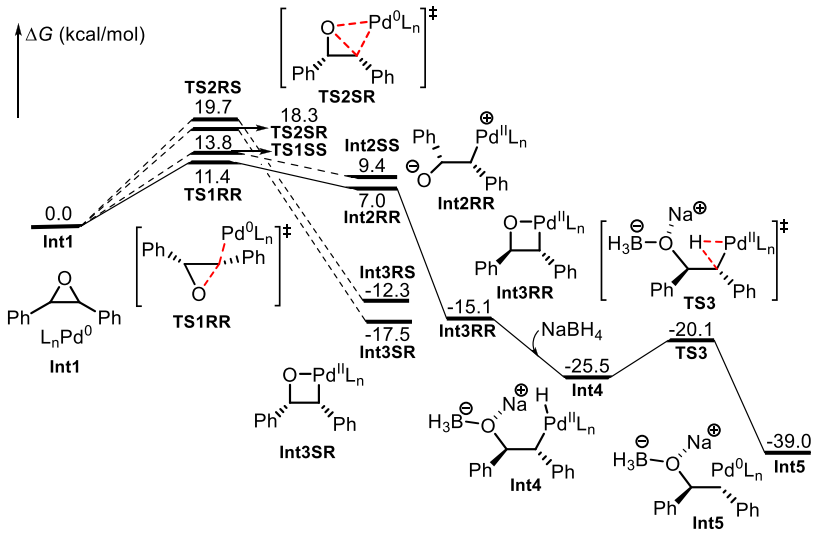

Figure 1. Potential energy surface of the Pd^0/Pd^{II} catalytic cycle.

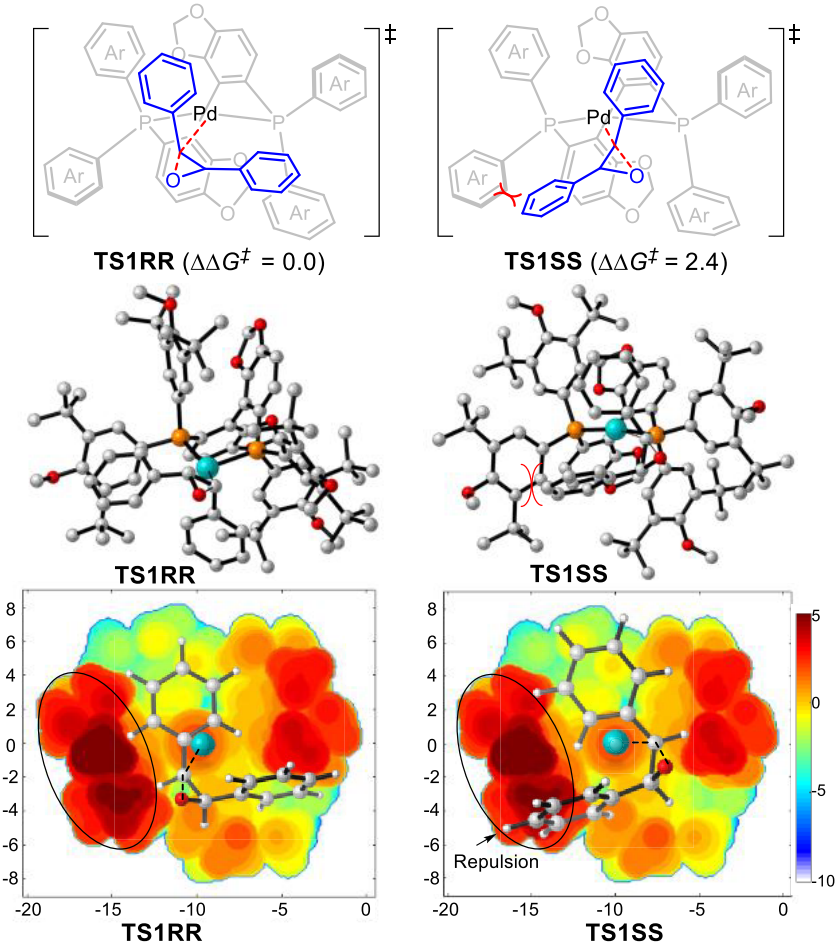

Figure 2. Three-dimensional structures and two-dimensional projection of key transition states **TS1RR** and **TS1SS**.

and 5% ee, which indicated that the ketone **3a** was not the intermediate (Scheme 6a). In addition, a labeling experiment was conducted using *cis*-2,3-d_2-**1b** as the starting material and delivered (−)-1,2-d_2-**2b** in 80% yield and 96% ee with the maintained deuteration rate of the benzylic site (Scheme 6b), which also excluded the formal hydrogenolysis mechanism.

Considering that palladium acetate has Lewis acidity, which might catalyze the ring-opening of epoxides as Lewis acid catalysts (see the Supporting Information for details), two control experiments were conducted. Trace amounts of the product were observed when sodium borohydride was used in the absence of a palladium catalyst (Scheme 6c). The reaction also did not occur when palladium acetate was used without

https://doi.org/10.1021/jacs.5c12776
J. Am. Chem. Soc. 2025, 147, 43560−43570

(*R*)-DTBM-SegPhos (Scheme 6d). Collectively, these data indicated that palladium acetate has low catalytic activity as a Lewis acid for the formal hydrogenolysis of *cis*-**1a**. According to literature reports,[13] palladium-catalyzed isomerization of epoxides usually underwent a Pd(0)/Pd(II)-catalyzed mechanism. The asymmetric hydrogenolysis of the epoxides in this work may also involve the Pd(0)/Pd(II) catalytic cycle. Some control experiments were carried out to verify this hypothesis. $Pd(P^tBu_3)_2$ was used as catalyst precursor and delivered (−)-**2a** with a similar reactivity and ee value as palladium acetate (Scheme 6e). When $Pd(P^tBu_3)_2$ was used without a chiral ligand, the product (±)-**2a** could be obtained in a low 22% yield (Scheme 6f). The above experimental results indicated that the hydrogenolysis is likely to proceed through a Pd(0)/Pd(II) mechanism.[18]

The mechanistic pathway was further investigated using density functional theory (DFT) at the M06*L*/6−311+G(d,p), SDD/IEF-PCM(DMF)//M06*L*/6−31G(d), and SDD/IEF-PCM (DMF) levels of theory to elucidate the full reaction process and the origin of the stereoselectivity (see the Supporting Information for details). As illustrated in Figure 1, the zerovalent palladium−ligand complex L_nPd^0 (**Int1**) was chosen as the zero point, and two possible oxidative addition pathways between L_nPd^0 and the substrate **1a** were evaluated. In the first pathway, the oxidative addition of **1a** to L_nPd^0 proceeds *via* transition states **TS1SS** ($\Delta G^{\ddagger}$ = 13.8 kcal/mol) and **TS1RR** ($\Delta G^{\ddagger}$ = 11.4 kcal/mol), yielding the cationic and anionic intermediates **Int2RR** and **Int2SS**, respectively. The intermediate **Int2RR** then isomerizes to form the more thermodynamically stable four-membered ring intermediate **Int3RR**. Alternatively, **1a** and L_nPd^0 can directly form the four-membered ring intermediates **Int3RS** and **Int3SR** *via* transition states **TS2RS** ($\Delta G^{\ddagger}$ = 19.7 kcal/mol) and **TS2SR** ($\Delta G^{\ddagger}$ = 18.3 kcal/mol), respectively. Computational analysis revealed that the pathway involving **TS1RR** is the most energetically favorable. Subsequently, **Int3RR** undergoes transmetalation in the presence of $NaBH_4$, generating the intermediate **Int4**. Finally, **Int4** undergoes reductive elimination *via* the transition state **TS3** ($\Delta G^{\ddagger}$ = 5.4 kcal/mol) to afford intermediate **Int5** and regenerates the L_nPd^0 catalyst, thereby completing the catalytic cycle. The agreement between theoretical calculations and experimental results regarding the absolute stereochemistry of (−)-(*S*)-**2a** or (−)-*d*-**2a** offers further support for an outer-sphere (S_N2-like) oxidative addition of L_nPd^0 onto the epoxide.

To elucidate the origin of stereoselectivity in the oxidative addition process, we systematically compared the key transition-state structures. As illustrated in Figure 2, the transition state **TS1SS** exhibits significant steric repulsion between the substrate **1a** and the substituents on the phosphine ligand, leading to a higher activation energy ($\Delta G^{\ddagger}$ = 13.8 kcal/mol) compared to **TS1RR** ($\Delta G^{\ddagger}$ = 11.4 kcal/mol). To further assess the influence of the ligand on chiral induction, the phosphine substituents in **TS1RR** and **TS1SS** were computationally replaced with hydrogen atoms. This modification reduced the energy difference between the transition states from 2.4 kcal/mol (Figure 2) to 0.7 kcal/mol (Figure S2), underscoring the critical role of the phosphine ligand in controlling the reaction selectivity. Additionally, two-dimensional projection analysis of the stereocontrolling transition states (**TS1RR** and **TS1SS**) was conducted. The results revealed stronger nonbonded repulsions between the ligand and the substrate in **TS1SS** than those in **TS1RR**, further confirming that the increased steric hindrance in **TS1SS** elevates its transition-state energy. Collectively, these analyses demonstrate that the substituents on the phosphine ligand are pivotal in determining the reaction's stereoselectivity.

Through the combination of experimental and theoretical studies, the following possible mechanism was proposed: first, the oxidative addition of the chiral Pd(0) complex with epoxide *cis*-**1a** generated the zwitterion species **A**, which further cyclized to afford the four-membered ring species **A′**. Next, species A′ conducted the fast hydrogen transfer in the presence of sodium borohydride to afford the active Pd−H species B. Finally, the product (−)-**2a** was obtained through reductive elimination and protonolysis. The chiral Pd(0) complex was regenerated to complete the catalytic cycle. Theoretical calculations revealed that the oxidative addition serves as both the rate-determining step and the enantioselectivity-determining step of the palladium-catalyzed hydrogenolysis process (Scheme 7).

Scheme 7. Plausible Mechanism

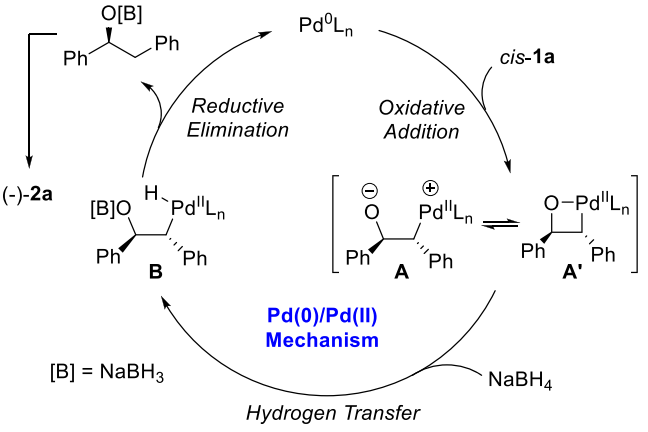

CONCLUSIONS

In summary, a palladium-catalyzed asymmetric hydrogenolysis of epoxides has been developed. The lynchpin is the suppression of the impact of adverse *β*-H elimination by the borane with good oxyphilicity as a hydride source to accelerate hydrogen transfer and the use of the bulky bidentate phosphine (*R*)-DTBM-SegPhos-based chiral palladium catalysts. The hydrogenolysis desymmetrization of *cis*-epoxides was achieved, giving a series of alcohols with excellent enantioselectivities, which also provided a good solution to the site-specific incorporation of deuterium in organic molecules. Trisubstituted epoxides were compatible under this catalytic system through kinetic resolution with up to a 58.9 selectivity factor. By the combination of experimental and theoretical studies, a plausible Pd(0)/Pd(II) catalytic mechanism was proposed. Further work on exploring this palladium catalytic system on other types of epoxides is ongoing in our laboratory, and we hope this work can inspire the development of new asymmetric transformations of epoxides with transition-metal catalysts.

https://doi.org/10.1021/jacs.5c12776
J. Am. Chem. Soc. 2025, 147, 43560−43570

■ ASSOCIATED CONTENT

Supporting Information

The Supporting Information is available free of charge at https://pubs.acs.org/doi/10.1021/jacs.5c12776.

Detailed experimental procedures, characterization of new compounds, and spectral and DFT data (PDF)

Accession Codes

Deposition Number 2327564 contains the supplementary crystallographic data for this paper. These data can be obtained free of charge via the joint Cambridge Crystallographic Data Centre (CCDC) and Fachinformationszentrum Karlsruhe Access Structures service.

■ AUTHOR INFORMATION

Corresponding Authors

Chang-Bin Yu − *State Key Laboratory of Catalysis, Dalian Institute of Chemical Physics, Chinese Academy of Sciences, Dalian 116023, P. R. China;* orcid.org/0000-0003-0247-9740; Email: cbyu@dicp.ac.cn

Yu Lan − *College of Chemistry, and Pingyuan Laboratory, Zhengzhou University, Zhengzhou, Henan 450001, P. R. China;* orcid.org/0000-0002-2328-0020; Email: lanyu@cqu.edu.cn

Yong-Gui Zhou − *State Key Laboratory of Catalysis, Dalian Institute of Chemical Physics, Chinese Academy of Sciences, Dalian 116023, P. R. China;* orcid.org/0000-0002-3321-5521; Email: ygzhou@dicp.ac.cn

Authors

Xiang Li − *State Key Laboratory of Catalysis, Dalian Institute of Chemical Physics, Chinese Academy of Sciences, Dalian 116023, P. R. China*

Qianqian Shi − *State Key Laboratory of Antiviral Drugs, and Pingyuan Laboratory, Henan Normal University, Xinxiang, Henan 453007, P. R. China*

Qing-Xian Xie − *State Key Laboratory of Catalysis, Dalian Institute of Chemical Physics, Chinese Academy of Sciences, Dalian 116023, P. R. China*

Huan Jing − *State Key Laboratory of Catalysis, Dalian Institute of Chemical Physics, Chinese Academy of Sciences, Dalian 116023, P. R. China*

Complete contact information is available at: https://pubs.acs.org/10.1021/jacs.5c12776

Notes

The authors declare no competing financial interest.

■ ACKNOWLEDGMENTS

We thank the National Key Research and Development Program of China (2023YFA1507500), the National Natural Science Foundation of China (22371276), and Dalian Institute of Chemical Physics (DICP I202103, I202241) for financial support.

■ REFERENCES

(1) (a) Chen, K.; Li, H.; Lei, Z.-Q.; Li, Y.; Ye, W.-H.; Zhang, L.-S.; Sun, J.; Shi, Z. J. Reductive Cleavage of the C_{sp2}-C_{sp3} Bond of Secondary Benzyl Alcohols: Rhodium Catalysis Directed by N-Containing Groups. *Angew. Chem., Int. Ed.* **2012**, *51*, 9851−9855. (b) Patra, T.; Agasti, S.; Modak, A.; Maiti, D. Nickel-Catalyzed Hydrogenolysis of Unactivated Carbon-Cyano Bonds. *Chem. Commun.* **2013**, *49*, 8362−8364. (c) Tobisu, M.; Nakamura, K.; Chatani, N. Nickel-Catalyzed Reductive and Borylative Cleavage of Aromatic Carbon-Nitrogen Bonds in *N*-Aryl Amides and Carbamates. *J. Am. Chem. Soc.* **2014**, *136*, 5587−5590. (d) Tam, C. M.; To, C. T.; Chan, K. S. Ligand Effect on the Rhodium Porphyrin Catalyzed Hydrogenation of [2.2]Para-cyclophane with Water: Key Bimetallic Hydrogenation. *Dalton Trans.* **2017**, *46*, 10057−10063. (e) Su, B.; Li, Y.; Li, Z. H.; Hou, J.-L.; Wang, H. Activation of C-C Bonds *via* σ-Bond Metathesis: Hydroborenium Catalyzed Hydrogenolysis of Cyclopropanes. *Organometallics* **2020**, *39*, 4159−4163. (f) Zhu, J.; Xue, Y.; Zhang, R.; Ratchford, B. L.; Dong, G. Catalytic Activation of Unstrained C(Aryl)-C(Alkyl) Bonds in 2,2′-Methylene-diphenols. *J. Am. Chem. Soc.* **2022**, *144*, 3242−3249. (g) Xu, Y.; Yang, Y.; Liu, Y.; Li, Z. H.; Wang, H. Boron-Catalysed Hydrogenolysis of Unactivated C(aryl)-C(alkyl) Bonds. *Nat. Catal.* **2023**, *6*, 16−22.

(2) (a) Alonso, F.; Beletskaya, I. P.; Yus, M. Metal-Mediated Reductive Hydrodehalogenation of Organic Halides. *Chem. Rev.* **2002**, *102*, 4009−4091. (b) Xue, F.; Xiong, J.; Chen, R.; Mo, G.; Peng, P.; Wang, Z. Research Progress on Dehalogenation Reaction. *Chin. J. Org. Chem.* **2013**, *33*, 2291−2297. (c) Whittlesey, M. K.; Peris, E. Catalytic Hydrodefluorination with Late Transition Metal Complexes. *ACS Catal.* **2014**, *4*, 3152−3159. (d) Eisenstein, O.; Milani, J.; Perutz, R. N. Selectivity of C-H Activation and Competition between C-H and C-F Bond Activation at Fluorocarbons. *Chem. Rev.* **2017**, *117*, 8710−8753. (e) Pilli, R.; Balakrishnan, V.; Chandrasekaran, R.; Rasappan, R. Iron-Catalyzed Protodehalogenation of Alkyl and Aryl Halides using Hydrosilanes. *Org. Biomol. Chem.* **2019**, *17*, 1749−1753. (f) Moore, J. T.; Lu, C. C. Catalytic Hydrogenolysis of Aryl C-F Bonds Using a Bimetallic Rhodium-Indium Complex. *J. Am. Chem. Soc.* **2020**, *142*, 11641−11646. (g) Li, M.-X.; Li, M.-L.; Tang, Y.-L.; Sun, Y.; Qu, L.; Huang, F.; Mao, Z.-W. Exploration of Cu-Catalyzed Regioselective Hydrodehalogenation of *o*-Haloanilides using EtOH as Hydrogen Source. *J. Organomet. Chem.* **2021**, *943*, No. 121844. (h) Jheng, N.-Y.; Ishizaka, Y.; Naganawa, Y.; Minami, Y.; Sekiguchi, A.; Iizuka, K.; Nakajima, Y. Radical Hydrodehalogenation of Aryl Halides with H_2 Catalyzed by a Phenanthroline-Based PNNP Cobalt(I) Complex. *ACS Catal.* **2022**, *12*, 2320−2329. (i) Burhenn, A.; Bavaro, R.; Gessner, V. H. Pd-Catalysed Hydrodehalogenation of Aryl Chlorides: A Mild Method for Deuteration and Detoxification. *Catal. Sci. Technol.* **2023**, *13*, 3545−3550.

(3) (a) van Engelen, M. C.; Teunissen, H. T.; de Vries, J. G.; Elsevier, C. J. Suitable Ligands for Homogeneous Ruthenium-Catalyzed Hydrogenolysis of Esters. *J. Mol. Catal. A: Chem.* **2003**, *206*, 185−192. (b) Revell, J. D.; Ganesan, A. A 'Triflate-Like' Tetrafluoroarylsulfonate Linker for Multifunctional Solid-Phase Organic Synthesis. *Chem. Commun.* **2004**, 1916−1917. (c) Sergeev, A. G.; Hartwig, J. F. Selective, Nickel-Catalyzed Hydrogenolysis of Aryl Ethers. *Science* **2011**, *332*, 439−443. (d) Kim, H. J.; Su, L.; Jung, H.; Koo, S. Selective Deoxygenation of Allylic Alcohol: Stereocontrolled Synthesis of Lavandulol. *Org. Lett.* **2011**, *13*, 2682−2685. (e) Tobisu, M.; Yamakawa, K.; Shimasakia, T.; Chatani, N. Nickel-Catalyzed Reductive Cleavage of Aryl-Oxygen Bonds in Alkoxy- and Pivaloxyarenes Using Hydrosilanes as a Mild Reducing Agent. *Chem. Commun.* **2011**, *47*, 2946−2948. (f) Herrmann, J. M.; König, B. Reductive Deoxygenation of Alcohols: Catalytic Methods Beyond Barton McCombie Deoxygenation. *Eur. J. Org. Chem.* **2013**, *2013*, 7017−7027. (g) Ren, Y.-L.; Tian, M.; Tian, X.-Z.; Wang, Q.; Shang, H.; Wang, J.; Zhang, Z. C. Highly Selective Reductive Cleavage of Aromatic Carbon-Oxygen Bonds Catalyzed by a Cobalt Compound. *Catal. Commun.* **2014**, *52*, 36−39. (h) Kusumoto, S.; Nozaki, K. Direct and Selective Hydrogenolysis of Arenols and Aryl Methyl Ethers. *Nat. Commun.* **2015**, *6*, No. 6296. (i) Wenz, J.; Wadepohl, H.; Gade, L. H. Regioselective Hydrosilylation of Epoxides Catalysed by Nickel(II) Hydrido Complexes. *Chem. Commun.* **2017**, *53*, 4308−4311. (j) Igarashi, T.; Haito, A.; Chatani, N.; Tobisu, M. Nickel-Catalyzed Reductive Cleavage of Carbon-Oxygen Bonds in Anisole Derivatives Using Diisopropylaminoborane. *ACS Catal.* **2018**, *8*, 7475−7483. (k) Li, J.; Wang, Z.-X. Nickel-Catalyzed C-O Bond Reduction of Aryl and Benzyl 2-Pyridyl Ethers. *Chem. Commun.* **2018**,

54, 2138−2141. (l) Ciszek, B.; Fleischer, I. Homogeneous Palladium-Catalyzed Transfer Hydrogenolysis of Benzylic Alcohols Using Formic Acid as Reductant. *Chem. - Eur. J.* **2018**, *24*, 12259−12263.
(4) (a) Liu, W.; Li, W.; Spannenberg, A.; Junge, K.; Beller, M. Iron-Catalysed Regioselective Hydrogenation of Terminal Epoxides to Alcohols under Mild Conditions. *Nat. Catal.* **2019**, *2*, 523−528. (b) Yao, C.; Dahmen, T.; Gansäuer, A.; Norton, J. *anti*-Markovnikov Alcohols *via* Epoxide Hydrogenation through Cooperative Catalysis. *Science* **2019**, *364*, 764−767. (c) Ye, K.-Y.; McCallum, T.; Lin, S. Bimetallic Radical Redox-Relay Catalysis for the Isomerization of Epoxides to Allylic Alcohols. *J. Am. Chem. Soc.* **2019**, *141*, 9548−9554. (d) Thiyagarajan, S.; Gunanathan, C. Ruthenium-Catalyzed Selective Hydrogenation of Epoxides to Secondary Alcohols. *Org. Lett.* **2019**, *21*, 9774−9778.
(5) (a) Liu, W.; Leischner, T.; Li, W.; Junge, K.; Beller, M. A General Regioselective Synthesis of Alcohols by Cobalt-Catalyzed Hydrogenation of Epoxides. *Angew. Chem., Int. Ed.* **2020**, *59*, 11321−11324. (b) Magre, M.; Paffenholz, E.; Maity, B.; Cavallo, L.; Rueping, M. Regiodivergent Hydroborative Ring Opening of Epoxides *via* Selective C-O Bond Activation. *J. Am. Chem. Soc.* **2020**, *142*, 14286−14294. (c) Steiniger, K. A.; Lambert, T. H. Primary Alcohols *via* Nickel Pentacarboxycyclopentadienyl Diamide Catalyzed Hydrosilylation of Terminal Epoxides. *Org. Lett.* **2021**, *23*, 8013−8017. (d) Tadiello, L.; Gandini, T.; Stadler, B. M.; Tin, S.; Jiao, H.; de Vries, J. G.; Pignataro, L.; Gennari, C. Regiodivergent Reductive Opening of Epoxides by Catalytic Hydrogenation Promoted by a (Cyclopentadienone)iron Complex. *ACS Catal.* **2022**, *12*, 235−246. (e) Thiyagarajan, S.; Gunanathan, C. Catalytic Hydrogenation of Epoxides to Alcohols. *Chem. Asian J.* **2022**, *17*, No. e202200118. (f) Head, M. C.; Joseph, B. T.; Keith, J. M.; Chianese, A. R. The Mechanism of Markovnikov-Selective Epoxide Hydrogenolysis Catalyzed by Ruthenium PNN and PNP Pincer Complexes. *Organometallics* **2023**, *42*, 347−356.
(6) Li, X.; Wang, G.-W.; Liu, L.-X.; Yu, C.-B.; Zhou, Y.-G. Palladium-Catalyzed Asymmetric Hydrogenolysis of Aryl Triflates for Construction of Axially Chiral Biaryls. *Angew. Chem., Int. Ed.* **2023**, *62*, No. e202301337.
(7) (a) Chan, A. S. C.; Coleman, J. P. Homogeneous Catalytic Asymmetric Hydrogenolysis of Sodium Epoxysuccinate: the First Example of Asymmetric Hydrogenolysis of an Epoxide. *J. Chem. Soc. Chem. Commun.* **1991**, 535−536. (b) Bakos, J.; Orosz, Á.; Cserépi, S.; Tóth, I.; Sinou, D. Chiral Sulfonated Phosphines. Rhodium(I)-Catalyzed Asymmetric Hydrogenolysis of Epoxides. *J. Mol. Catal. A* **1997**, *116*, 85−97.
(8) Chen, J.; Zhang, Z.; Liu, D.; Zhang, W. Palladium-Catalyzed Chemo- and Enantioselective C-O Bond Cleavage of α-Acyloxy Ketones by Hydrogenolysis. *Angew. Chem., Int. Ed.* **2016**, *55*, 8444−8447.
(9) (a) Chen, M.-W.; Chen, Q.-A.; Duan, Y.; Ye, Z.-S.; Zhou, Y.-G. Asymmetric Hydrogenolysis of Racemic Tertiary Alcohols, 3-Substituted 3-Hydroxyisoindolin-1-Ones. *Chem. Commun.* **2012**, *48*, 1698−1700. (b) Yu, C.-B.; Zhou, Y.-G. Palladium-Catalyzed Asymmetric Hydrogenolysis of N-Sulfonyl AminoAlcohols via Achiral Enesulfonamide Intermediates. *Angew. Chem., Int. Ed.* **2013**, *52*, 13365−13368. (c) Song, B.; Yu, C.-B.; Huang, W.-X.; Chen, M.-W.; Zhou, Y.-G. Formal Palladium-Catalyzed Asymmetric Hydrogenolysis of Racemic N-Sulfonyl- oxaziridines. *Org. Lett.* **2015**, *17*, 190−193.
(10) (a) Zhou, J.-Q.; Sheng, W.-J.; Jia, J.-H.; Ye, Q.; Gao, J.-R.; Jia, Y.-X. Chiral Phosphoric Acid Catalyzed Asymmetric Hydrogenolysis of Racemic 3-Aryl-3-Hydroxyisoindolin-1-Ones. *Tetrahedron Lett.* **2013**, *54*, 3082−3084. (b) Yin, Q.; Wang, S.-G.; You, S.-L. Asymmetric Synthesis of Tetrahydro-β-Carbolines *via* Chiral Phosphoric Acid Catalyzed Transfer Hydrogenation Reaction. *Org. Lett.* **2013**, *15*, 2688−2691. (c) Ge, C.; Liang, R.-X.; Liu, R.-R.; Xiang, B.; Jia, Y.-X. Ir(I)-Catalyzed Enantioselective Hydrogenolysis of 3-Aryl-3-Hydroxyisoindolin-1-Ones. *Tetrahedron Lett.* **2017**, *58*, 142−144. (d) Li, Y.; Wan, M.; Sun, S.; Fu, Z.; Huang, H.; Liu, L. Efficient Access to Chiral Benzo[c]chromenes via Asymmetric Transfer Hydrogenation of Ketals. *Org. Chem. Front.* **2018**, *5*, 1280−1283. (e) Zhang, Y.; He, L.; Shi, L. Asymmetric Hydrogenolysis of Racemic 3-Substitued-3-Hydroxyisoindolin-1-Ones Employing SPINOL-Derived Chiral Phosphoric Acid. *Tetrahedron Lett.* **2018**, *59*, 1592−1595. (f) Zheng, J.; Jongcharoenkamol, J.; Peters, B. B. C.; Guhl, J.; Ponra, S.; Ahlquist, M. S. G.; Andersson, P. G. Iridium-Catalysed Enantioselective Formal Deoxygenation of Racemic Alcohols *via* Asymmetric Hydrogenation. *Nat. Catal.* **2019**, *2*, 1093−1100. (g) Yan, Q.; Duan, M.; Chen, C.; Deng, Z.; Wu, M.; Yu, P.; He, M.-L.; Zhu, G.; Houk, K. N.; Sun, J. Organocatalytic Discrimination of non-Directing Aryl and Heteroaryl Groups: Enantioselective Synthesis of Bioactive Indole-Containing Triarylmethanes. *Chem. Sci.* **2022**, *13*, 5767−5773. (h) Han, Z.; Zang, Y.; Liu, C.; Guo, W.; Huang, H.; Sun, J. Enantioselective Synthesis of Triarylmethanes via Organocatalytic Transfer Hydrogenation of para-Quinone Methides. *Chem. Commun.* **2022**, *58*, 7128−7131.
(11) (a) Nielsen, L. P. C.; Jacobsen, E. N. *Aziridines and Epoxides in Organic Synthesis*; Yudin, A. K., Ed.; Wiley-VCH: Weinheim, Germany, 2006; pp 7−9. (b) Wang, P.-A. Organocatalyzed Enantioselective Desymmetrization of Aziridines and Epoxides. *Beilstein J. Org. Chem.* **2013**, *9*, 1677−1695. (c) da Silva, A. R.; dos Santos, D. A.; Paixão, M. W.; Corrêa, A. G. Stereoselective Multicomponent Reactions in the Synthesis or Transformations of Epoxides and Aziridines. *Molecules* **2019**, *24*, No. 630. (d) Zhan, X.; Du, X. Regio- and Enantioselective Epoxy Ring Opening of 2,3-Epoxy-3-phenyl Alcohols/Carbox- ylic Acids and Their Derivatives. *Russ. J. Org. Chem.* **2020**, *56*, 679−692. (e) Moschona, F.; Savvopoulou, I.; Tsitopoulou, M.; Tataraki, D.; Rassias, G. Epoxide Syntheses and Ring-Opening Reactions in Drug Development. *Catalysts* **2020**, *10*, No. 1117. (f) Lidskog, A.; Li, Y.; Wärnmark, K. Asymmetric Ring-Opening of Epoxides Catalyzed by Metal-Salen Complexes. *Catalysts* **2020**, *10*, No. 705. (g) Du, Q.; Zhang, L.; Gao, F.; Wang, L.; Zhang, W. Progress in Transition Metal-Catalyzed Asymmetric Ring-Opening Reactions of Epoxides and Aziridines. *Chin. J. Org. Chem.* **2022**, *42*, 3240−3262.
(12) (a) Heravi, M. M.; Asadi, S.; Nazari, N.; Lashkariani, B. M. Application of Corey-Bakshi-Shibata, Corey-Kim, Corey-Seebach, Corey-Winter, Corey-Link, and Corey-Ganem-Gilman in Organic and Total Synthesis. *Monatsh. Chem.* **2016**, *147*, 961−987. (b) Abdul Fattah, T.; Saeed, A. Applications of Keck Allylation in the Synthesis of Natural Products. *New J. Chem.* **2017**, *41*, 14804−14821. (c) Heravi, M. M.; Lashaki, T. B.; Fattahi, B.; Zadsirjan, V. Application of Asymmetric Sharpless Aminohydroxylation in Total Synthesis of Natural Products and Some Synthetic Complex Bioactive Molecules. *RSC Adv.* **2018**, *8*, 6634−6659. (d) Gonela, U. M.; Yadav, J. S. Synthesis of Chiral Propargyl Alcohols Following the Base-Induced Elimination Protocol: Application in the Total Synthesis of Natural Products. *New J. Chem.* **2020**, *44*, 4972−4986. (e) Zhang, Y.-L.; Zhao, Z.-N.; Li, W.-L.; Li, J.-J.; Kalita, S. J.; Schneider, U.; Huang, Y.-Y. Catalytic Asymmetric Aldehydeprenylation and Application in the Total Synthesis of (−)-Rosiridol and (−)-Bifurcadiol. *Chem. Commun.* **2020**, *56*, 10030−10033. (f) Boiarska, Z.; Braga, T.; Silvani, A.; Passarella, D. Brown Allylation: Application to the Synthesis of Natural Products. *Eur. J. Org. Chem.* **2021**, *2021*, 3214−3222. (g) Bowen, J. I.; Wang, L.; Crump, M. P.; Willis, C. L. Synthetic and Biosynthetic Methods for Selective Cyclisations of 4,5-Epoxy Alcohols to Tetrahydropyrans. *Org. Biomol. Chem.* **2022**, *20*, 1150−1175. (h) Štiblariková, M.; Lásiková, A.; Gracza, T. Benzyl Alcohol/Salicylaldehyde-Type Poly-ketide Metabolites of Fungi: Sources, Biosynthesis, Biological Activities, and Synthesis. *Mar. Drugs* **2023**, *21*, No. 19.
(13) (a) Kulasegaram, S.; Kulawiec, R. J. Palladium-Catalyzed Isomerization of Aryl-Substituted Epoxides: a Selective Synthesis of Substituted Benzylic Aldehydes and Ketones. *J. Org. Chem.* **1997**, *62*, 6547−6561. (b) Kulasegaram, S.; Kulawiec, R. J. On the Mechanism of the Palladium(0)-Catalyzed Isomerization of Epoxides to Carbonyl Compounds. *Tetrahedron* **1998**, *54*, 1361−1374. (c) Muzart, J. Pd-Mediated Reactions of Epoxides. *Eur. J. Org. Chem.* **2011**, 4717−4741. (d) Huang, C.-Y.; Doyle, A. G. The Chemistry of Transition Metals

https://doi.org/10.1021/jacs.5c12776
J. Am. Chem. Soc. 2025, 147, 43560−43570

with Three-Membered Ring Heterocycles. *Chem. Rev.* **2014**, *114*, 8153−8198.
(14) Süsse, L.; Hermeke, J.; Oestreich, M. The Asymmetric Piers Hydrosilylation. *J. Am. Chem. Soc.* **2016**, *138*, 6940−6943.
(15) (a) Chung, J. Y. L.; Mancheno, D.; Dormer, P. G.; Variankaval, N.; Ball, R. G.; Tsou, N. N. Diastereoselective Friedel-Crafts Alkylation of Indoles with Chiral α-Phenyl Benzylic Cations. Asymmetric Synthesis of *anti*-1,1,2-Triarylalkanes. *Org. Lett.* **2008**, *10*, 3037−3040. (b) Lou, S.; Fu, G. C. Nickel/Bis(oxazoli- ne)-Catalyzed Asymmetric Kumada Reactions of Alkyl Electrophiles: Cross-Couplings of Racemic α-Bromoketones. *J. Am. Chem. Soc.* **2010**, *132*, 1264−1266. (c) Henriques, D. S. G.; Zimmer, K.; Klare, S.; Meyer, A.; Rojo-Wiechel, E.; Bauer, M.; Sure, R.; Grimme, S.; Schiemann, O.; Flowers II, R. A.; Gansäuer, A. Highly Active Titanocene Catalysts for Epoxide Hydrosilylation: Synthesis, Theory, Kinetics, EPRS Pectroscopy. *Angew. Chem., Int. Ed.* **2016**, *55*, 7671−7675.
(16) CCDC 2327564 contains supplementary crystallographic data of compound (+)-**5d**.
(17) (a) Gansäuer, A.; Bluhm, H.; Pierobon, M. Emergence of a Novel Catalytic Radical Reaction: Titanocene-Catalyzed Reductive Opening of Epoxides. *J. Am. Chem. Soc.* **1998**, *120*, 12849−12859. (b) Gansäuer, A.; Lauterbach, T.; Bluhm, H.; Noltemeyer, M. A Catalytic Enantioselective Electron Transfer Reaction: Titanocene-Catalyzed Enantioselective Formation of Radicals from meso-Epoxides. *Angew. Chem., Int. Ed.* **1999**, *38*, 2909−2910. (c) Gansäuer, A.; Bluhm, H. Reagent-Controlled Transition-Metal-Catalyzed Radical Reactions. *Chem. Rev.* **2000**, *100*, 2771−2788. (d) Gansäuer, A.; Bluhm, H.; Lauterbach, T. Titanocene-Catalysed Enantioselective Opening of meso-Epoxides. *Adv. Synth. Catal.* **2001**, *343*, 785−787. (e) Gansäuer, A.; Lauterbach, T.; Narayan, S. Strained Heterocycles in Radical Chemistry. *Angew. Chem., Int. Ed.* **2003**, *42*, 5556−5573. (f) Gansäuer, A.; Bluhm, H.; Rinker, B.; et al. Reagent-Controlled Stereoselectivity in Titanocene-Catalyzed Epoxide Openings: Reductions and Intermolecular Additions to α,β-Unsaturated Carbonyl Compounds. *Chem. - Eur. J.* **2003**, *9*, 531−542. (g) Gansäuer, A.; Fan, C.-A.; Keller, F.; Karbaum, P. Regiodivergent Epoxide Opening: a Concept in Stereoselective Catalysis Beyond Classical Kinetic Resolutions and Desymmetrizations. *Chem. - Eur. J.* **2007**, *13*, 8084−8090. (h) Gansäuer, A.; Fan, C.-A.; Keller, F.; Keil, J. Titanocene-Catalyzed Regiodivergent Epoxide Openings. *J. Am. Chem. Soc.* **2007**, *129*, 3484−3485. (i) Gansäuer, A.; Karbaum, P.; Schmauch, D.; Einig, M.; Shi, L.; Anoop, A.; Neese, F. Titanocene-Catalyzed Regiodivergent Epoxide Openings. *Chem. - Asian J.* **2014**, *9*, 2289−2294. (j) Funken, N.; Mühlhaus, F.; Gansäuer, A. General, Highly Selective Synthesis of 1,3- and 1,4-Difunctionalized Building Blocks by Regiodivergent Epoxide Opening. *Angew. Chem., Int. Ed.* **2016**, *55*, 12030−12034. (k) Weißbarth, H.; Mühlhaus, F.; Gansäuer, A. Titanocene-Catalyzed Regiodivergent Epoxide Opening from Desymmetrizing meso-Epoxides to Regiodivergent Arylation of Epoxides. *Synthesis* **2020**, *52*, 2940−2947. (l) Gansäuer, A. From Enantioselective to Regiodi- vergent Epoxide Opening and Radical Arylation-Useful or Just Interesting. *Synlett* **2021**, *32*, 447−456. (m) Li, S.; Zhu, H.; Li, L.; Chen, W.; Jiang, J.; Qu, Z.-W.; Grimme, S.; Zhang, Y.-Q. A Nuclearity-Dependent Enantiodivergent Epoxide Opening via Enthalpy-Controlled Mononuclear and Entropy-Controlled Dinuclear (salen)titanium Catalysis. *Angew. Chem., Int. Ed.* **2023**, *62*, No. e202309525. (n) Li, L.; Yang, S.; Xu, Z.; Li, S.; Jiang, J.; Zhang, Y.-Q. Dinuclear Titanium(III)-Catalyzed Radical-Type Kinetic Resolution of Epoxides for the Enantioselective Synthesis of cis-Glycidic Esters. *J. Am. Chem. Soc.* **2024**, *146*, 13546−13557.
(18) (a) Kündig, E. P.; Chaudhuri, P. D.; House, D.; Bernardinelli, G. Catalytic Enantioselective Hydrogenolysis of [$Cr(CO)_3$(5,8-dibromonaphthalene)]. *Angew. Chem., Int. Ed.* **2006**, *45*, 1092−1095. (b) Mercier, A.; Yeo, W. C.; Chou, J.; Chaudhuri, P. D.; Bernardinelli, G.; Kündig, E. P. Synthesis of Highly Enantiomerically Enriched Planar Chiral Ruthenium Complexes via Pd-Catalysed Asymmetric Hydrogenolysis. *Chem. Commun.* **2009**, 5227−5229. (c) Mercier, A.; Yeo, W. C.; Urbaneja, X.; Kündig, E. P. An Efficient Entry to Planar Chiral Organometallic Complexes via Pd-Catalyzed Asymmetric Hydrogenolysis. *Chimia* **2010**, *64*, 177−179. (d) Mercier, A.; Urbaneja, X.; Yeo, W. C.; Chaudhuri, P. D.; Cumming, G. R.; House, D.; Bernardinelli, G.; Kündig, E. P. Asymmetric Catalytic Hydrogenolysis of Aryl-Halide Bonds in Fused Arene Chromium and Ruthenium Complexes. *Chem. - Eur. J.* **2010**, *16*, 6285−6299. (e) Hirai, M.; Terada, S.; Yoshida, H.; Ebine, K.; Hirata, T.; Kitagawa, O. Catalytic Enantioselective Synthesis of N-C Axially Chiral Mebroqualone and Its Derivatives through Reductive Asymmetric Desymmetrization. *Org. Lett.* **2016**, *18*, 5700−5703.

https://doi.org/10.1021/jacs.5c12776
J. Am. Chem. Soc. 2025, 147, 43560−43570